Transactions, SMiRT-25
Charlotte, NC, USA, August 4-9, 2019
Division VII

DEVELOPMENT OF SEISMIC COUNTER MEASURES AGAINST CLIFF EDGES FOR ENHANCEMENT OF COMPREHENSIVE SAFETY OF NUCLEAR POWER PLANTS
PART 8: IDENTIFICATION AND ASSESSMENT OF CLIFF EDGES OF NPP STRUCTURAL SYSTEM

Akemi Nishida[1], Byunghyun Choi[2], Hidemasa Yamano[3], Tatsuya Itoi[4] and Tsuyoshi Takada[5]

[1] Senior Principal Researcher, Japan Atomic Energy Agency, Japan (nishida.akemi@jaea.go.jp)
[2] Researcher, Japan Atomic Energy Agency, Japan
[3] Group Leader, Japan Atomic Energy Agency, Japan
[4] Associate Professor, The University of Tokyo, Japan
[5] Professor, The University of Tokyo, Japan

ABSTRACT

Assessments of cliff edge effects are crucial for nuclear power plants (NPPs). The objective of this study is to identify and quantify possible cliff edge effects through a seismic safety evaluation of an NPP, based on the concepts of risk and defense in depth. Cliff edges of both physical- and knowledge-oriented types are considered in this study. We investigated the seismic isolation effect for physical cliff edges, and the difference in modeling methods of the target structure for knowledge-oriented cliff edges. Response analysis was performed using a sway-rocking (SR) model and a three-dimensional model of the target building. The seismic isolation effect of the base-isolated building was confirmed by comparing with results of earthquake-resistant buildings. Differences in results between the SR model and the three-dimensional model were confirmed. Failure probabilities were assessed using these response analysis results. Results are presented and discussed herein.

INTRODUCTION

Cliff-edge effects of nuclear power plants (NPPs) have received significant attention particularly after the Fukushima Daiichi NPP accident. The objective of this study is to assess cliff edge effects, which are crucial for NPPs. This study identifies and quantifies possible cliff edge effects through a seismic safety evaluation of an NPP, based on the concepts of risk and defense in depth. Cliff edges of both physical- and knowledge-oriented types are considered in this study.

We herein discuss issues relevant to cliff edges in an NPP building system. To examine how the cliff edge state is specified and evaluated in the seismic response analysis of a building system, we investigated the seismic isolation mechanism that was primarily related to physical cliff edges and the modeling effects of a building system that was primarily related to knowledge-oriented cliff edges. Response analysis was performed to identify potential physical cliff edges in a base-isolated building and to explore the effects of base-isolation in reducing the response. The seismic isolation effect of the base-isolated building was confirmed by comparing with results of earthquake-resistant buildings. Meanwhile, a potential knowledge-oriented cliff edge was identified in the spatial distribution of the building responses by the differences between the results from the SR model and three-dimensional model. This was not considered in the conventional SR model, but it is expected to be quantified using a three-dimensional model. In particular, we quantitatively evaluated the uncertainty within the same floor by calculating from the analytical results using a three-dimensional building model. Furthermore, we attempted to evaluate the failure probability (fragility) of the target building under certain limited conditions. Results are presented and discussed herein.

TWO TYPES OF CLIFF EDGES

In this study, cliff edges of both physical- and knowledge-oriented types were considered (Takada (2017)). Table 1 shows examples of cliff edges to be considered for a building system. We first focused on the avoidance of cliff edges related to a base-isolated building system.

Table 1: Examples of cliff edges to be considered for the building system

Physical Cliff Edge	Knowledge-oriented cliff edge
Damage to plant building and equipment, foundation lifting, sliding, nonlinear effects, collision with retaining wall of base-isolated building, etc.	Behavior in non-target region of modeling, behavior in region where knowledge and experience are insufficient, e.g., a strongly nonlinear region.

CLIFF EDGES OF A BUILDING SYSTEM

The introduction of a seismic isolation system significantly reduces the building response, and the physical cliff edge of a normal earthquake-resistant building is expected to be avoided. Moreover, the behavior of the base-isolated building is expected to remain within the linear elastic region at levels of input ground motion that produce nonlinear behaviors in an earthquake-resistant building. Consequently, the elastic design of equipment becomes possible, thus improving the accuracy of design evaluation. However, as the input level further increases, other types of physical cliff edges may appear. In other words, it can be regarded as the physical cliff edges of a base-isolated building. The physical cliff edges of a base-isolated building may include damage to the base-isolation device and collision with the retaining wall.

In this study, we assumed that two types of physical cliff edge events occurred for our seismic response analysis. The first cliff edge should be discussed based on whether the maximum shear strain of the earthquake-resistant building exceeds 4000 μ. However, even if the input ground motion level is 3000 gal, the building maintained its strength. The second cliff edge will be discussed as collision with a retaining wall for the base-isolated building. Physical cliff edge problems primarily involve knowledge-oriented cliff edge problems. Herein, we discuss the difference between the results from the SR model and three-dimensional model.

INPUT GROUND MOTION

As shown in Figure 1, two types of simulated ground motions were used as inputs. Input ground motion A, comprising three components, was generated using the empirical Green function method for earthquakes with specified source faults; meanwhile, input ground motion B, comprising two components, was generated using a response spectrum method. The maximum acceleration of each wave was based on the basic earthquake ground motion level (before 2010 in Japan). Details are given in Nishida (2018).

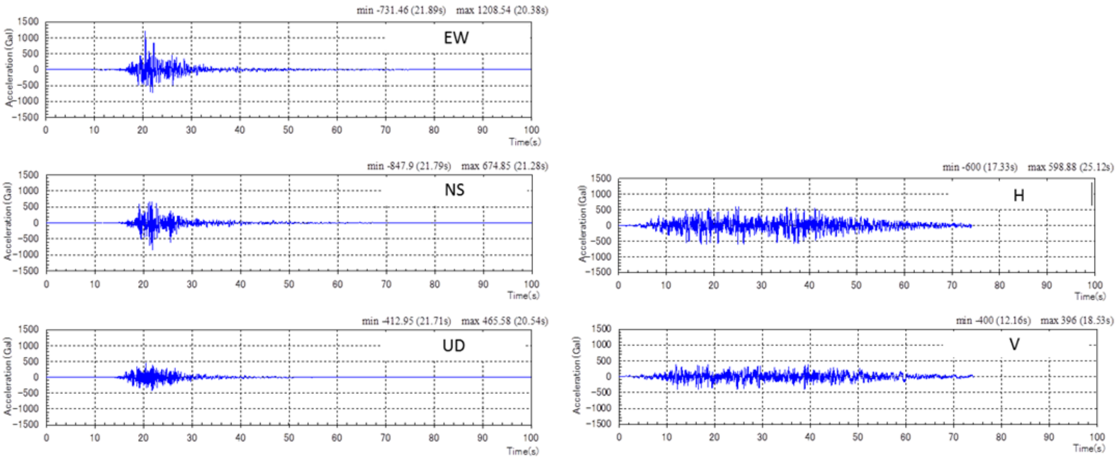

(a) Input ground motion A (three axes) (b) Input ground motion B (H-V2 axes)

Figure 1. Input ground motion used in the analysis (Nishida (2018))

ANALYSIS MODEL

Summary of reactor building modeling

After a literature survey of plant information, we obtained information from the KARISMA benchmark by the IAEA over a period of five years from 2008 until 2013 (IAEA TECDOC (2013)). Subsequently, we constructed an analytical model of the model plant using the information from the KARISMA benchmark.

The reactor building to be analyzed is 56.6 m (NS) × 59.6 m (EW), the height is 63.4 m, and the height from the ground surface is 37.7 m. Seismic response analysis to consider the effect of a seismic isolation system was be performed using the SR model and three-dimensional FE model. The SR model was created based on public information and literature and confirmed to be consistent with the results (TEPCO, 2009). In this section, we summarize the construction of the three-dimensional FE model. The details are given in reference Nishida (2018).

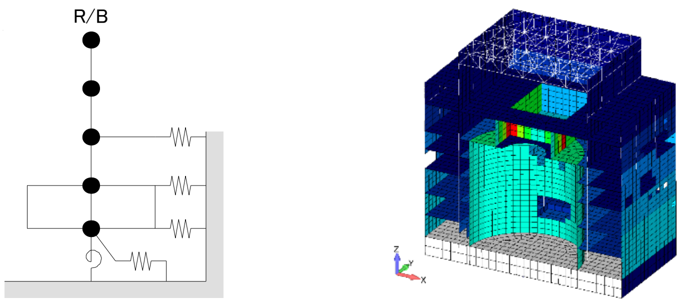

(a) Sway Rocking (SR) model (b) three-dimensional FE model

Figure 2. Examples of nuclear building model (Nishida (2018))

The model comprises 14,334 elements, 11,796 nodes, and ~64,000 degrees of freedom. Figure 2 shows the SR model and FE model of the reactor building. For setting the nonlinear properties of the reinforced concrete in the three-dimensional model, the Maekawa model (Maekawa (1999)) was used for the shell elements of the earthquake-resistant wall and auxiliary wall, and the peak pressure strain was set to 3000 μ such that the initial inclination was equal to Young's modulus. The damping of the three-dimensional model was set to 5% at the second natural frequency of the SR model.

Soil–structure interactions (SSIs) are represented by spring elements in the conventional manner. The springs for the FE model were arranged by distributing the springs of the SR model along the interacting surfaces of the wall or the base mat.

Validation of analytical model

To verify the constructed analytical models, an eigenvalue analysis was performed, and the results of the FE and SR models were compared. The obtained natural frequencies are listed in Table 2. It has been confirmed that global modes such as mode 1 or mode 2 are almost equivalent though local modes higher than mode 3 are different (Nishida (2015)).

Table 2: Natural frequencies (NS)

	SR model				3D FE model			
mode	Natural Freq. (Hz)	Natural period (sec)	Effective mass ratio		Natural Freq. (Hz)	Natural period (sec)	Effective mass ratio	
			X	RZ			X	RZ
1	2.278	0.439	0.756	0.096	2.268	0.441	0.778	0.000
2	5.172	0.193	0.240	0.354	5.158	0.194	0.161	0.000

To validate the constructed FE model, we compared the analytical results to the observed earthquake data. The results indicated that the observed and analytical results were primarily consistent (Nishida (2015)). We confirmed that the results were sufficiently accurate to use this model to perform seismic response analysis.

Analytical model with seismic isolation system

A base-isolated system installed to the building was modeled as distributed springs. The seismic isolation hysteresis characteristic of the SR model and three-dimensional model were defined as the normal bilinear model equivalent to the hysteresis characteristics of a lead rubber bearing (LRB). The properties of the seismic isolation device were set referring to Asahara (2016) and Shima (2016).

ANALYTICAL CONDITION

For comparison, analyses were performed for an earthquake-resistant building model. Seismic response analysis was performed on two types of input ground motion described in the previous section. To compare the analytical results of the SR model and three-dimensional model, one directional input wave with an N–S direction component or U–D direction component was used for the analyses. Analytical results using an input wave with the N–S direction component are shown herein.

ANALYTICAL RESULTS

Response analyses of the SR model and the three-dimensional model were performed using input ground motions A and B. The detailed analytical results were given in reference MEXT (2017).

Comparison of analytical results from SR model and three-dimensional model

(1) Earthquake-resistant building

Figure 3 shows the distribution of the maximum N–S shear strain under input ground motion A from the SR model and three-dimensional model of an earthquake-resistant building. The analysis results obtained when the input acceleration was changed to 1, 2, and 3 times are shown in Figures 3 (a), (b), and (c), respectively. Although the results of the three-dimensional model contain large variations on each floor, it was confirmed that no major damage occurred on each earthquake-resistant wall. From the evaluation perspective, the maximum value of each floor should be used for evaluation; however, from the viewpoint of evaluating the fragility, the median of the values of each element for each floor is calculated and shown as red lines in the figure.

The maximum shear strain remained within the allowable range at the original load (shown in Figure 3 (a)), and the results from the SR model were close to the median values of those obtained from the three-dimensional model. In the floor responses below the first floor of the building, the median value of the results obtained from the three-dimensional model was confirmed to be lower than that from the SR model. However, the median value from the three-dimensional model is larger than that from the SR model in the upper layer of the building. The reason is considered that the out-of-plane deformation of the wall under the roof truss of the building increased the shear strain on the wall perpendicular to the deformed wall on the upper floor of the building. This suggests that a knowledge-oriented cliff edge may appear when the evaluation is conducted using an SR model, as the three-dimensional effect is not considered. These differences increase with the load level.

Focusing on the analytical results of the three-dimensional model, the tendency of shear strain distribution is different in each layer; furthermore, it is found that the variation is large from the basement to the 2nd floor. It is also confirmed that the results obtained using the SR model globally captured the trend of the results obtained using the three-dimensional model.

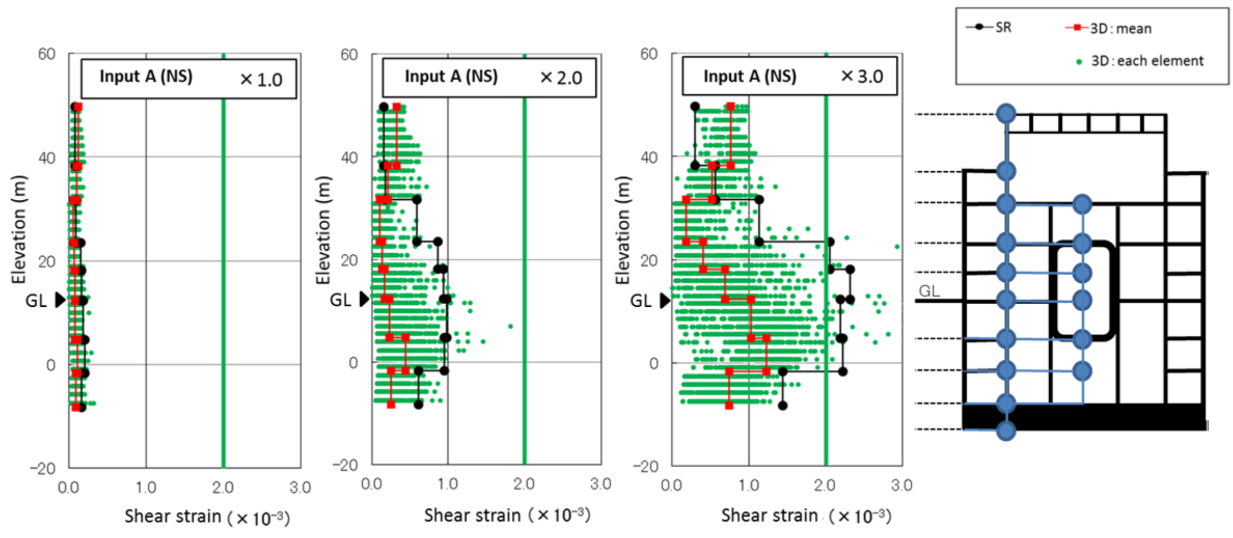

(a) Input x 1 (b) Input x 2 (c) Input x 3

Figure 3. Maximum shear strain from SR model and three-dimensional model (Nishida (2018))
Input ground motion A (N–S) (Differences by input acceleration level)

(2) Comparison of results between SR model and three-dimensional model

Figure 4 shows the distribution of the maximum N–S shear strain under thrice the input ground motion A from the SR model and three-dimensional model. The analytical results obtained using the earthquake-resistant model, base-isolated model with no collision, and base-isolated model with collision are shown in Figures 4 (a), (b), and (c), respectively. Moreover, in the analytical result obtained using the three-dimensional model, the seismic isolation effect can be confirmed, as well as the result of the SR model. However, in the three-dimensional model, the shear strain varies within the same layer, and the strain value that is likely to partially reach 2000 μ in the base-isolated building can be confirmed. This tendency is the same regardless of whether the possibility of a collision is considered.

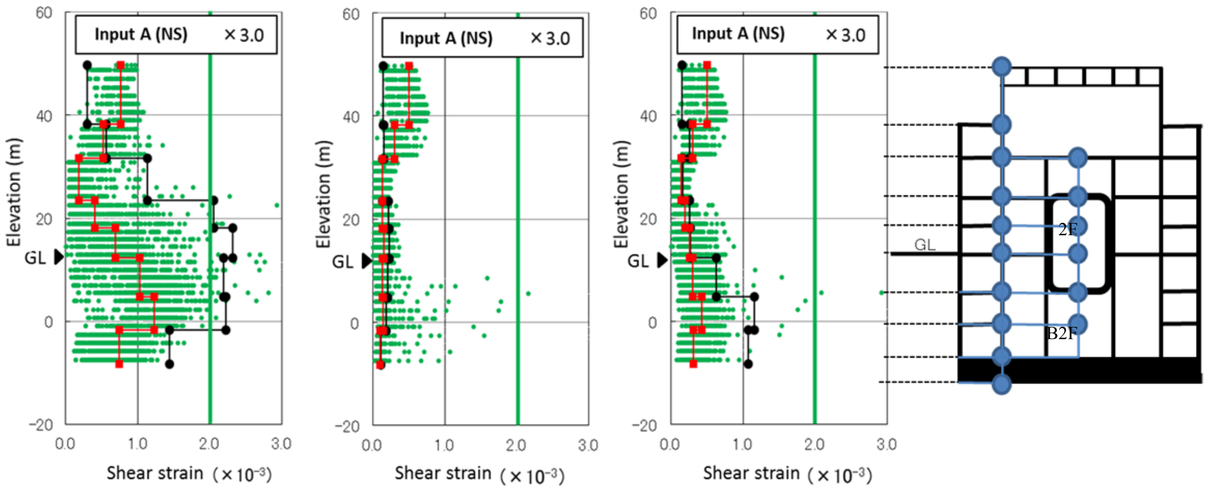

(a) Earthquake-resistant (b) Base-isolated (no collision) (c) Base-isolated (with collision)

Figure 4. Maximum shear strain from SR model and three-dimensional model (Nishida (2018))
Input ground motion A (N–S) (Differences by structural system)

Fragility evaluation of building system

(1) Evaluation of variation based on analysis results of three-dimensional model of building

Prior to the fragility evaluation, the variation in response was evaluated using the analysis results for the input scale 1 to 5 times the input acceleration A (NS). Although it is not realistic to calculate the building responses for four or five times the input ground motion A, we performed the calculation to make a fragility assessment of the building. The logarithm standard deviation for the median value of each layer of the three-dimensional model and the response ratio of the three-dimensional model to the SR model are shown in Figures 5 and 6, respectively. The logarithm standard deviation with respect to the median value of each building layer is ~0.4 on all layers, and it can be confirmed that the earthquake-resistant building tends to exhibit a greater difference in each layer than the seismic isolation building. The response ratio is smaller than that in the lower part and greater than that in the upper part. Similar to the results of the prior section, the difference in value of each layer is larger in the earthquake-resistant building than in the seismic isolated building.

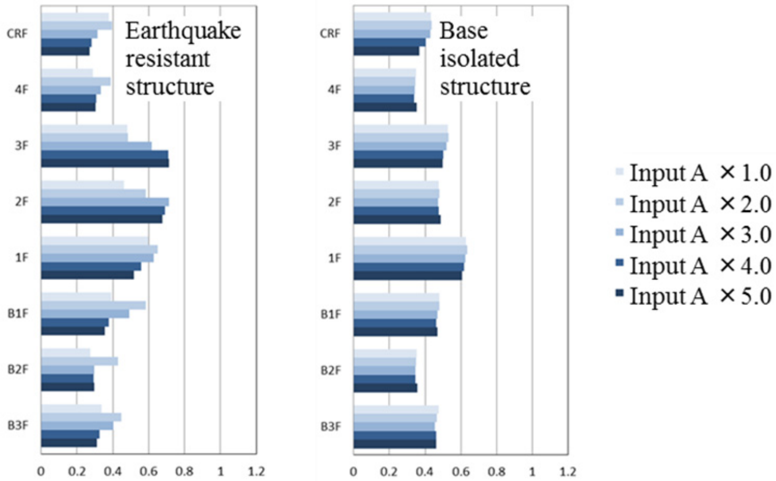

(a) Earthquake resistant (b) Base isolated

Figure 5. Logarithm standard deviation to the median of maximum shear strain from three-dimensional model: Input ground motion A (N–S)

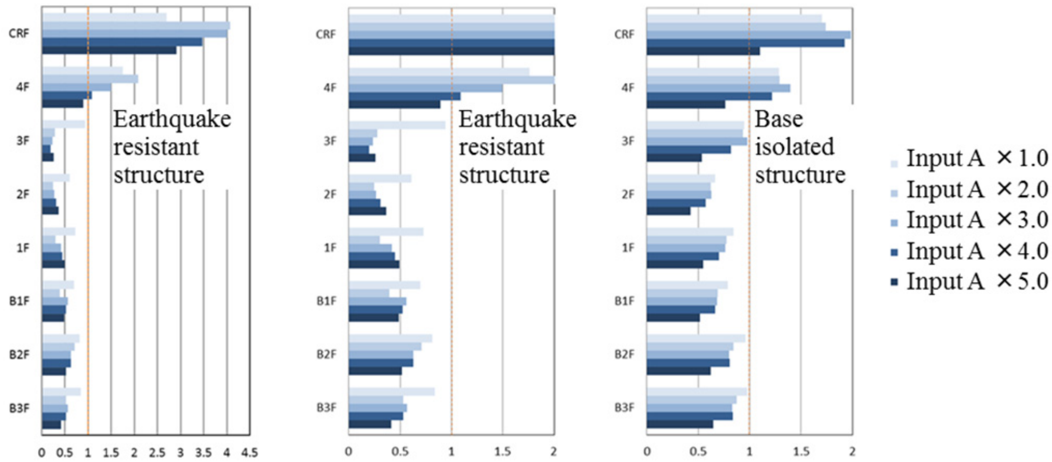

(a) Earthquake-resistant (Full scale) (b) Earthquake-resistant (c) Base-isolated

Figure 6. Response ration of maximum shear strain (Median of 3D FE model / SR model) : Input ground motion A (N–S)

(2) Trial of fragility evaluation

Fragility evaluation was performed in each layer of the building system based on the analysis results using the three-dimensional model and SR model for 1 to 5 times of input acceleration A (NS). In this study, we focused on the maximum shear strain of the walls to evaluate the fragility of the building system.

Figure 7 shows an example of the fragility curve calculated using the median of the SR model and three-dimensional model. The assumptions of the evaluation are also shown in Figure 7. From the figure, the cliff edge in the case of evaluation using an SR model is two to three times that of the horizontal axis Ss and indicates the possibility of avoiding by evaluating the building using a three-dimensional model.

Figure 8 shows an example of the B1F fragility curve calculated using the result of the SR model and each element (outer wall) of the three-dimensional model. From the figure, when the variation of each layer is considered, the SR model can produce a conservatively reasonable evaluation result. However, the element-by-element fragility curve does not indicate damage to the layer, but only local damages; therefore, a detailed analysis is required in the future.

Assumption:
・Median of the response: response of input ground motion
・Logarithm S.D. of response: 0.3
・Median of resistance: shear strain 5300μ
・Logarithm S.D. of resistance: 0.3

Assuming that the response and the input ground motion PGA can be approximated by the following equation, a fragility curve is evaluated as a lognormal distribution.

$$\log Y = p \cdot \log a + q$$

Y: response, a: input ground motion PGA

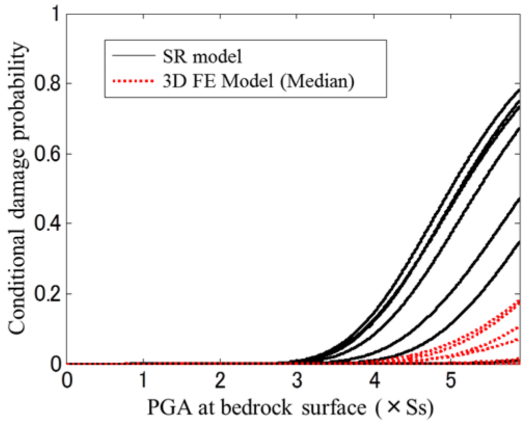

Figure 7. Fragility curve of each building layer:
Input ground motion A (N–S)

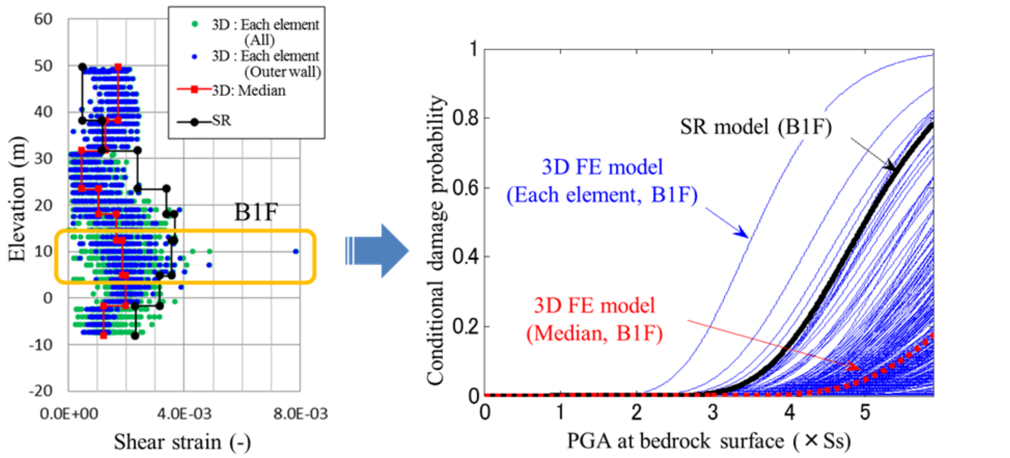

Figure 8. Fragility curve in each element of the three-dimensional model (B1F, outer wall)
Input ground motion A (N–S)

CONCLUSIONS

Possible cliff edges in NPP building systems were identified in this study. Cliff edges of both physical- and knowledge-oriented types were considered in this study. Furthermore, we created a preliminary study of methods to avoid the identified cliff edges.

Response analysis was performed to identify potential physical cliff edges in a base-isolated building and to explore the effect of base-isolation in reducing the response. The seismic isolation effect of the base-isolated building was confirmed by comparing with results of earthquake-resistant buildings. Furthermore, in the case of collision with the retaining wall of a base-isolated building, the level of damage was found to depend on the modeling of the collision condition assumed. This result suggested that by installing an appropriate energy absorber, the effects of collision can be mitigated in the future.

Meanwhile, a potential knowledge-oriented cliff edge was identified in the spatial distribution of the responses of the building walls by the differing results between the SR model and three-dimensional model. This was not considered in the conventional SR model, but it is expected to be quantified using a three-dimensional model. However, it is necessary to validate the analytical results of the three-dimensional model in a nonlinear region before quantifying the results.

Fragility evaluation was also performed using the response analysis results. The results indicated the possibility of avoiding the cliff edges of the SR model by evaluating the building using a three-dimensional model.

In future studies, we intend to further explore techniques for avoiding the cliff edge effects identified herein and evaluate fragility in more detail.

ACKNOWLEDGMENTS

The present study is supported by the project of “Development of Seismic Countermeasures against Cliff Edges for Enhancement of Comprehensive Safety of Nuclear Power Plants” entrusted to The University of Tokyo by the Ministry of Education, Sports, Science and Technology (MEXT).

REFERENCES

The Ministry of Education, Sports, Science and Technology (MEXT), (2017), “Development of Seismic Countermeasures against Cliff Edges for Enhancement of Comprehensive Safety of Nuclear Power Plants”, The research report of FY2017, The Initiatives for Atomic Energy Basic and Generic Strategic Research, The Center of World Intelligence Project for Nuclear S&T and Human Resource Development, (in Japanese).

Takada, T., et al. (2017), “Development of Seismic Countermeasures Against Cliff Edges for Enhancement of Comprehensive Safety of NPPs - Part 1: Conceptual Study on Identification and Avoidance of Cliff Edges of NPPs Against Earthquakes”, *Proc., SMiRT-24*, Busan, Korea.

Nishida, A., et al. (2018), “Development of Seismic Countermeasures against Cliff Edges for Enhancement of Comprehensive Safety of Nuclear Power Plants – Cliff Edges Relevant to NPP Building System –, Proc. PVP2018, Prague, Czech Republic.

IAEA TECDOC (2013), “Review of Seismic Evaluation Methodologies for Nuclear Power Plants Based on a Benchmark Exercise”, Technical report, No 1722.

Maekawa, K., et al. (1999), “Re-formulation of Spatially Averaged RC Constitutive Model with Quasi-orthogonal Bi-directional Cracking”, No.634, Vol.45, pp.157-176, (in Japanese).

TEPCO HD Co., Ltd. (2009), "Report on Seismic Safety Assessment Results (Rev. 1) at Kashiwazaki Kariwa Nuclear Power Station Unit 7 in accordance with the revision of the "Seismic Design Review Guidelines for Nuclear Power Plant”.

Nishida, A., et al. (2015), “Reliability Enhancement of Seismic Risk Assessment of NPP as Risk Management Fundamentals, - Part III: Sensitivity Analysis for the Quantification of Epistemic Uncertainty on Fragility Assessment”, Proc., SMiRT-23, Manchester, United Kingdom.

Asahara, S., et al. (2016), “Development of seismic isolation technology for nuclear plant - Part 33: Overview of developments - Part 2: Design and Evaluation of Seismic Isolation Building”, Summaries of technical papers of annual meeting, Architectural Institute of Japan, (in Japanese).

Shima T., et al. (2016), “Development of seismic isolation technology for nuclear plant - Part 34: Overview of developments - Part 3: Residual Risk Assessment”, Summaries of technical papers of annual meeting, Architectural Institute of Japan, (in Japanese).